



Supplement of

Aerosol–cloud–radiation interaction during Saharan dust episodes: the dusty cirrus puzzle

Axel Seifert et al.

Correspondence to: Axel Seifert (axel.seifert@dwd.de)

The copyright of individual parts of the supplement might differ from the article licence.

1 List of Saharan dust episodes

Figure S1 gives an overview of the mineral dust episodes in 2021 and 2022 (up to and including July 2022). The list of episodes is based on the operational German ceilometer network. The 2nd and 3rd column are the intensity and the maximum height of the dust layer based on the ceilometer backscatter data. Columns 5-7 are from five AERONET stations in Germany (Hohenpeissenberg, Lindenberg, Leipzig, Munich and Mainz). Given is the maximum coarse mode AOD at any of the 5 stations and the corresponding values of total AOD and Angstrom exponent (440-870 nm). The ICON-ART maximum dust AOD is the maximum of the simulated AOD of the global ICON-ART dust forecasting system taken at 9 Ceilometer stations in Germany (Hohenpeissenberg, Lindenberg, Leipzig, Weihenstephan, Mannheim, Würzburg, Stuttgart, Schleswig, Karlsruhe).

This list of dust episodes shows that the six cases presented in the paper are good candidates for interesting aerosol-cloud events and the occurrence of a 'dusty cirrus'. Indicators are high AOD and high maximum dust height. We could have exchanged the 27 April 2022 to 1 May 2022 with the event 28-30 March 2022, which has a deeper dust layer, or with 12-14 April 2022. We decided for the April-May episode, because we had some indications for aerosol-cloud-radiation effects for this case that we did not see for the other events. This is why we opted for that case. Most other mineral dust cases were either too weak or too shallow to be relevant for this study.

2 Validation using surface station data (Ceilometer, Pyranometer)

The retrieval of solar irradiance at the surface from the CERES instrument on board the Aqua and Terra satellites can be challenging in cloudy conditions. Hence, it is desirable to complement the satellite-based validation by the use of surface stations. DWD operates a network of 25 pyranometers in Germany, which can be used for this purpose. Due to the rather short time periods of 5 days we refrain from a decomposition in clear-sky and cloudy for the pyranometer data. Dusty conditions are defined based on ICON-D2-ART dust AOD exceeding 0.1. Figure S2 shows the results for all dust episodes investigated in this study.

DWD also operates a ceilometer network in Germany. Ceilometers are ground-based remote sensing instruments that provide profile-based information on cloud base heights over time. This allows a height-resolved validation of cloud fraction, with the limitation, that cirrus clouds can only be detected properly in the absence of dense clouds below the cirrus. Figure S3 presents the validation results of seven representative stations from DWD's ceilometer network for the period 1-5 March 2021. All simulations except ACI-dusty show a strong underestimation of cirrus cloud fraction in 7-10 km height (Fig. S3a). This underestimation is eliminated by ACI-dusty thanks to the newly developed dusty cirrus parameterization, which leads to a corresponding improvement in the height-resolved MAE (Fig. S3b). Likewise, the overall bias and MAE, accumulated over all height levels, is strongly improved by the ACI-dusty simulation whereas no significant difference exists between the other three simulations. These results support the conclusions based on satellite data as presented in the main paper. As the investigation of cirrus clouds during the other two dusty cirrus events is hindered by widespread mid- and low-level clouds, we refrain from using ground-based ceilometer data for a validation of these events.

3 Statistical evaluation for all 6 cases

Figures S4-S9 show the bias and MAE for each of the six Saharan dust episodes similar to Figs. 6. Here the reflected shortwave at TOA is always shown that has been dropped from Figs. 14, 17 of the paper. Figure S10 shows the statistics of all 6 dust episodes as Fig. 18 of the paper, but here including the reflected shortwave at TOA.

Figure S11 shows the error statistics for individual CERES footprints of outgoing long-wave radiation (OLR) as a function of the mineral dust AOD as predicted by ICON-D2-ART.

4 Auxillary plots

Figure S12 shows an Aqua overpass for the dusty cirrus case of 3 March 2021. Similarly, Figure S13 shows an Aqua overpass for the dusty cirrus case of 6 May 2022.

A comparison with radiosonde measurements for the dusty cirrus case of 3 March 2021 is shown in Figs. S14-S16. The in situ measurements show a good agreement with the ACI-dusty simulation.

Period based on Ceilometer data	Intensity based on Ceilometer data	Dust Max Height [km]	ICON-ART max DAOD	AERONET total AOD	AERONET max coarse AOD	AERONET min Angstrom Exp.
2021						
05.02.2021-06.02.2021	medium/ extreme	5	0.55	missing	missing	missing
21.02.2021-26.02.2021	medium/ strong	8	0.97	0.64	0.57	0.02
02.03.2021-04.03.2021	strong	8	0.62	0.56	0.38	0.43
08.03.2021-09.03.2021	weak	8	0.11	missing	missing	missing
28.03.2021-30.03.2021	weak	6	0.21	0.16	0.13	0.25
31.03.2021-02.04.2021	medium	6	0.30	0.65	0.44	0.39
04.04.2021-05.04.2021	weak	8	0.27	0.30	0.15	0.88
17.04.2021-21.04.2021	medium	7	0.24	0.29	0.16	1.00
17.06.2021-21.06.2021	medium/ strong	5	0.44	0.50	0.38	0.37
11.07.2021-14.07.2021	medium	5	0.41	0.35	0.22	0.64
16.07.2021-20.07.2021	weak	9	0.17	0.26	0.14	0.79
23.07.2021-25.07.2021	weak	5	0.22	0.57	0.29	1.03
25.09.2021-26.09.2021	medium	5	0.22	missing	missing	missing
2022						
15.03.2022-19.03.2022	extreme	10	0.83	missing	missing	missing
20.03.2022-25.03.2022	weak/ medium	10	0.26	missing	missing	missing
28.03.2022-30.03.2022	medium	10	0.36	missing	missing	missing
12.04.2022-14.04.2022	strong	6	0.44	0.57	0.44	0.16
18.04.2022-21.04.2022	weak	8	0.33	0.15	0.11	1.23
27.04.2022-03.05.2022	medium	4	0.33	0.47	0.24	0.60
04.05.2022-09.05.2022	medium	7	0.36	0.41	0.15	1.45
15.05.2022-16.05.2022	weak	4	0.34	0.21	0.11	0.78
18.05.2022-20.05.2022	weak	8	0.43	0.17	0.13	0.34
22.05.2022-23.05.2022	weak	5	0.50	missing	missing	missing
03.06.2022-05.06.2022	weak	6	0.26	0.24	0.20	0.29
15.06.2022-16.06.2022	weak	4	0.15	missing	missing	missing
17.06.2022-21.06.2022	medium	7	0.43	0.70	0.50	0.06
22.06.2022-23.06.2022	weak	4	0.24	missing	missing	missing
26.06.2022-30.06.2022	weak	7	0.30	0.31	0.24	0.44
03.07.2022-04.07.2022	weak	5	0.11	missing	missing	missing
17.07.2022-23.07.2022	medium	7	0.17	0.33	0.12	1.29

Figure S1. List of mineral dust episodes based on selected observations from DWD's operational ceilometer network over Germany and AERONET stations. The 6 cases of the paper are marked with yellowish color and bold font. The reddish color indicates events with a minimum intensity level of medium, based on ceilometer data (see text for details).

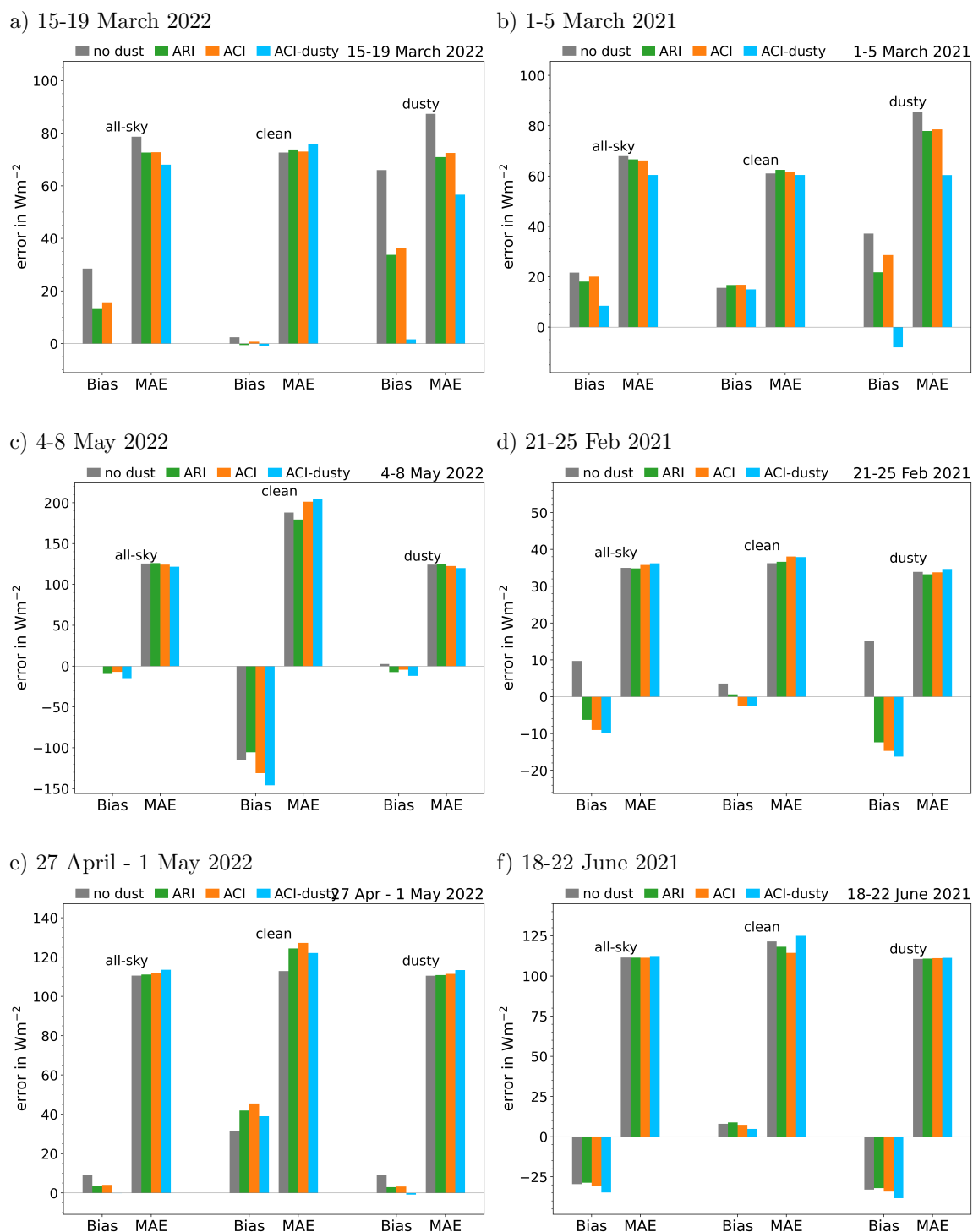
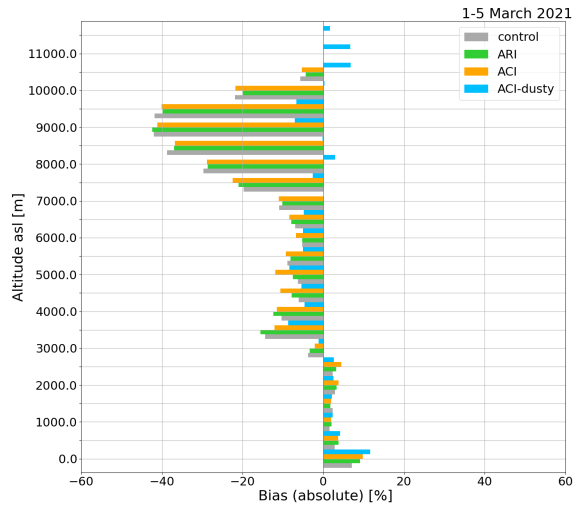
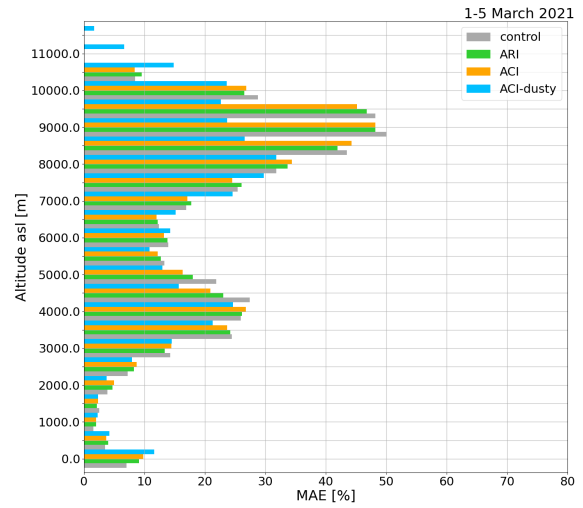


Figure S2. Validation of solar irradiance at the surface using DWD's pyranometer network for the six individual dust episodes

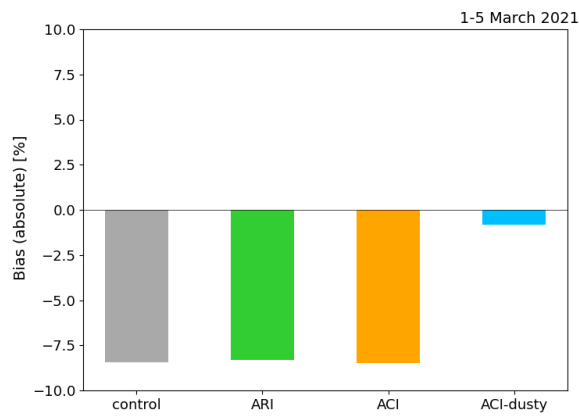
a) Bias (ceilometer profile)



b) MAE (ceilometer profile)



c) Bias (all heights)



d) MAE (all heights)

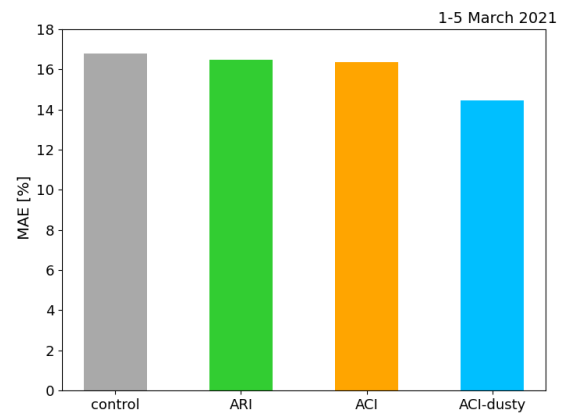
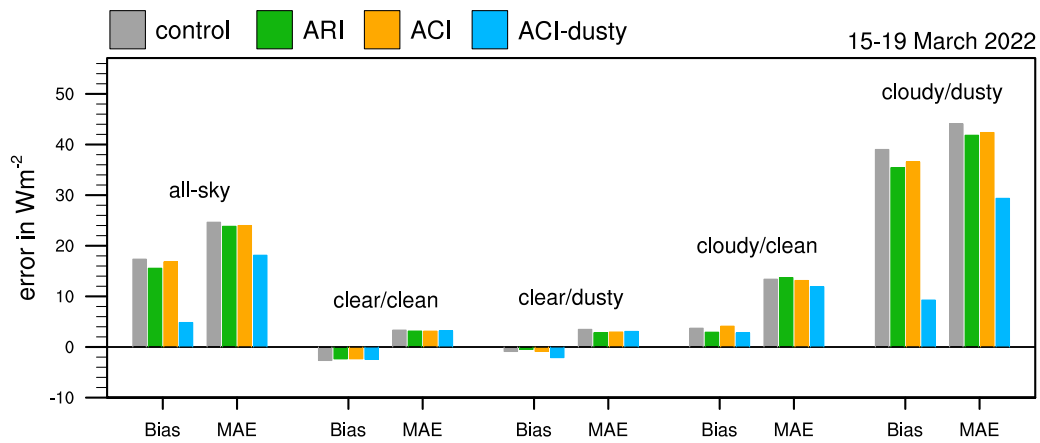
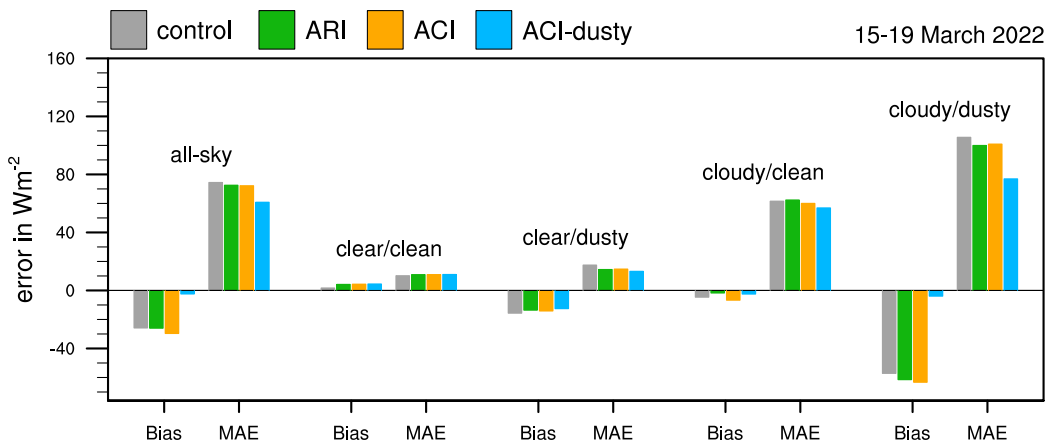


Figure S3. Validation of cloud fraction with ceilometer data of 7 representative stations in Germany (Hohenpeissenberg, Lindenberg, Leipzig, Stuttgart, Oberschleissheim, Meiningen, and Konstanz) during the dusty cirrus event from 1-5 March 2021. To focus on the dusty cirrus occurrence, we use ICON-ART AOD greater 0.1 as a filter.

a) ICON-ART vs CERES outgoing longwave radiation at TOA



b) ICON-ART vs CERES reflected shortwave radiation at TOA



c) ICON-ART vs CERES downward shortwave radiation at the surface

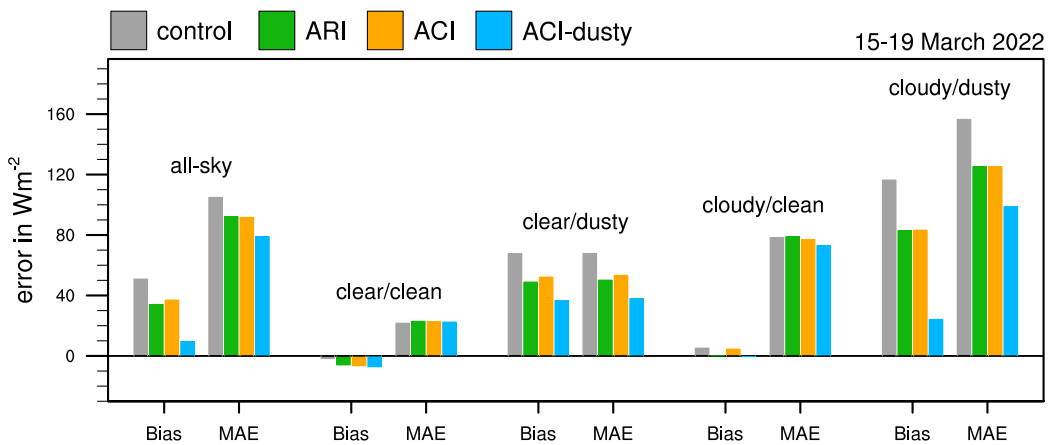
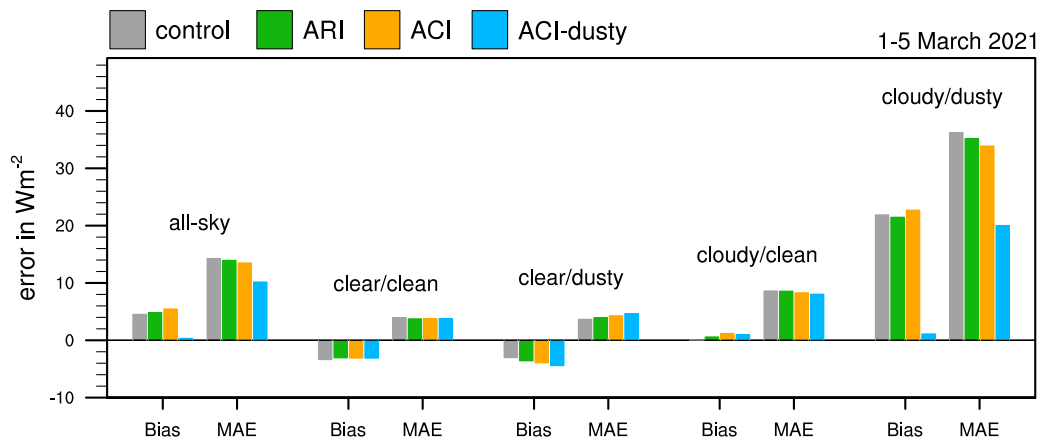
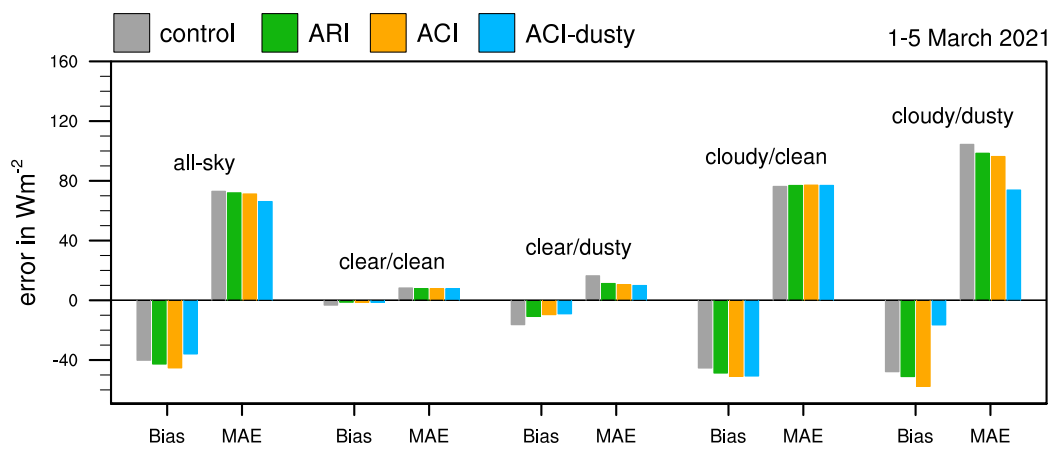


Figure S4. Bias and mean absolute error (MAE) of ICON-ART compared to CERES SSF level 2 radiative fluxes for 15-19 March 2022. Shown are the outgoing longwave radiation at the top of atmosphere (TOA), the reflected shortwave at TOA and to solar irradiance at the surface (from top to bottom)

a) ICON-ART vs CERES outgoing longwave radiation at TOA



b) ICON-ART vs CERES reflected shortwave radiation at TOA



c) ICON-ART vs CERES downward shortwave radiation at the surface

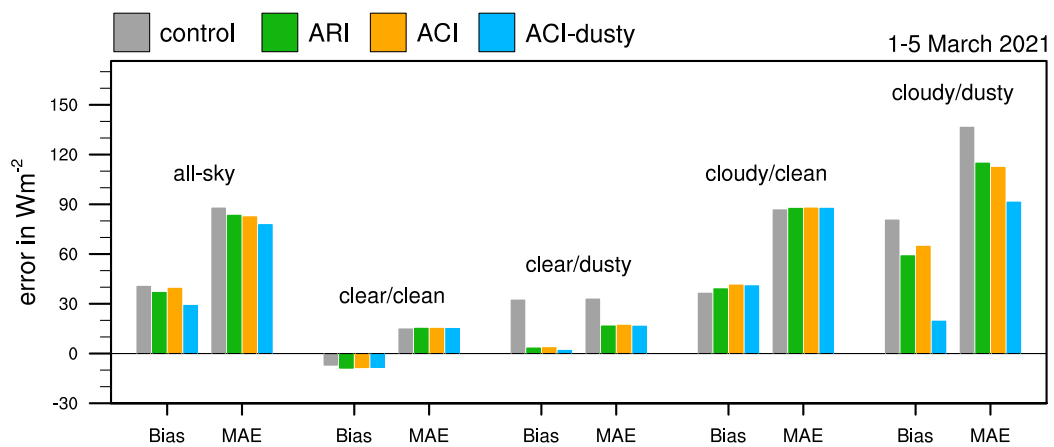
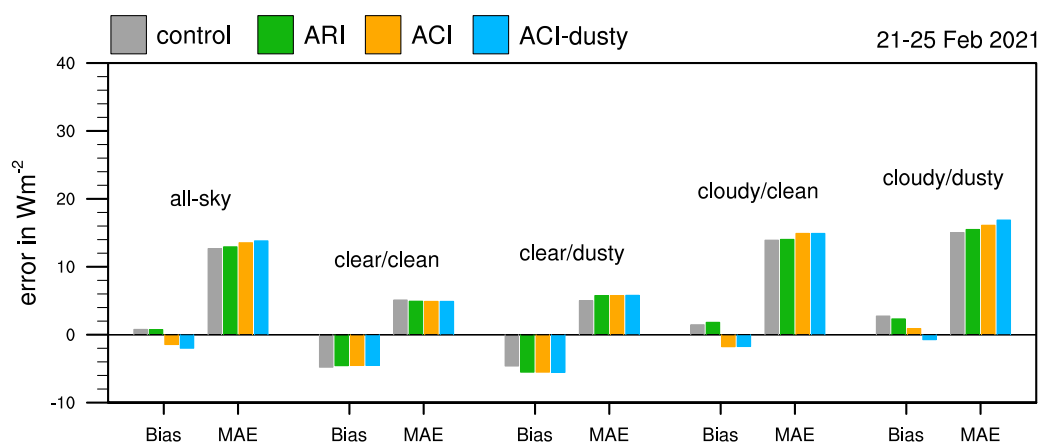
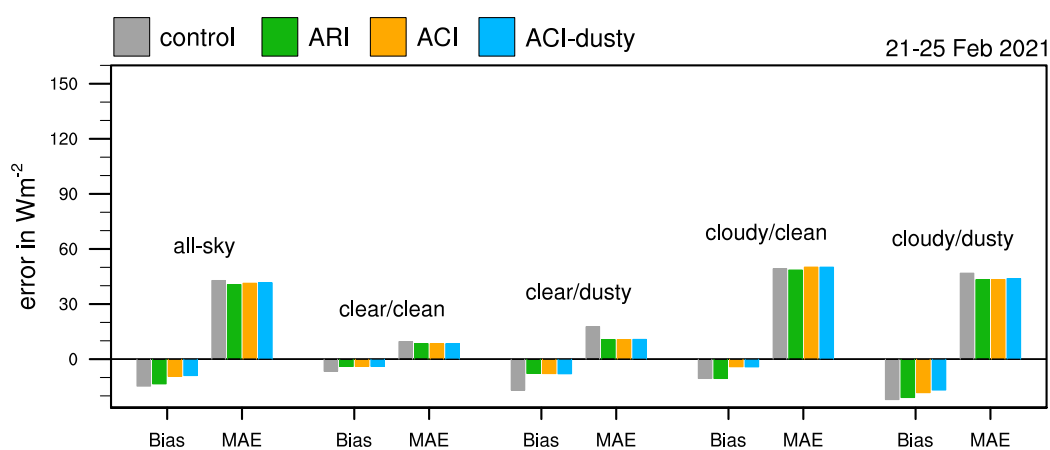


Figure S5. Bias and mean absolute error (MAE) of ICON-ART compared to CERES SSF level 2 radiative fluxes for 1-5 March 2021. Shown are the outgoing longwave radiation at the top of atmosphere (TOA), the reflected shortwave at TOA and to solar irradiance at the surface (from top to bottom)

a) ICON-ART vs CERES outgoing longwave radiation at TOA



b) ICON-ART vs CERES reflected shortwave radiation at TOA



c) ICON-ART vs CERES downward shortwave radiation at the surface

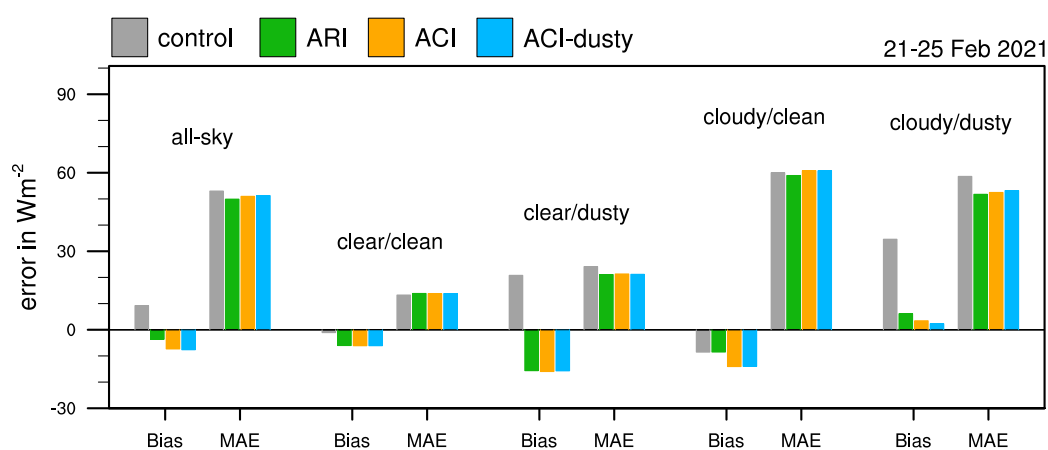
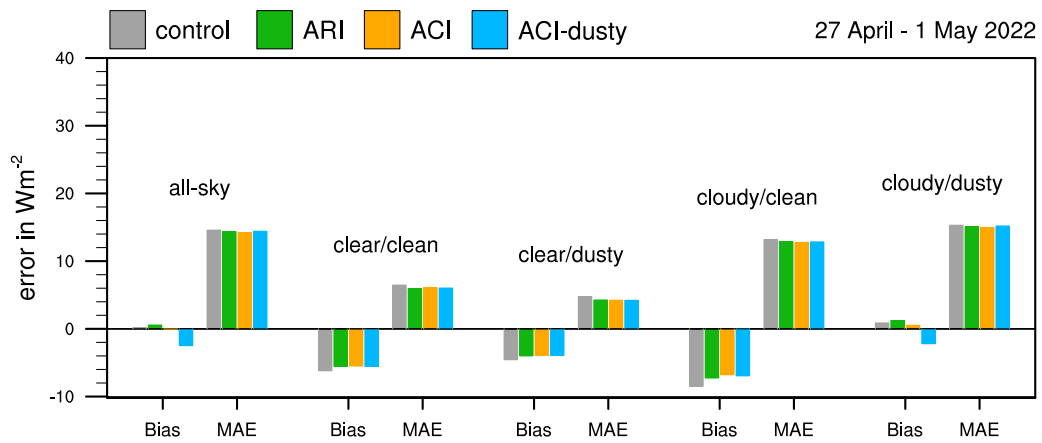
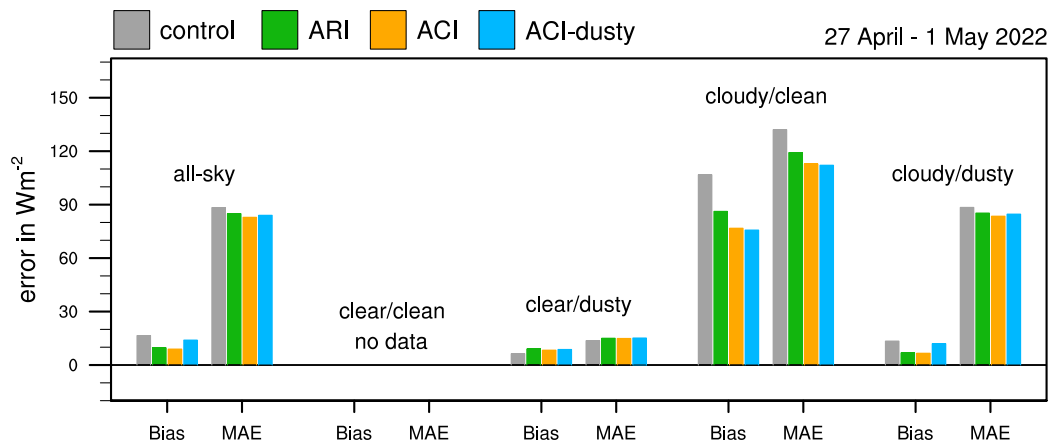


Figure S6. Bias and mean absolute error (MAE) of ICON-ART compared to CERES SSF level 2 radiative fluxes for 21-25 Feb 2021. Shown are the outgoing longwave radiation at the top of atmosphere (TOA), the reflected shortwave at TOA and to solar irradiance at the surface (from top to bottom)

a) ICON-ART vs CERES outgoing longwave radiation at TOA



b) ICON-ART vs CERES reflected shortwave radiation at TOA



c) ICON-ART vs CERES downward shortwave radiation at the surface

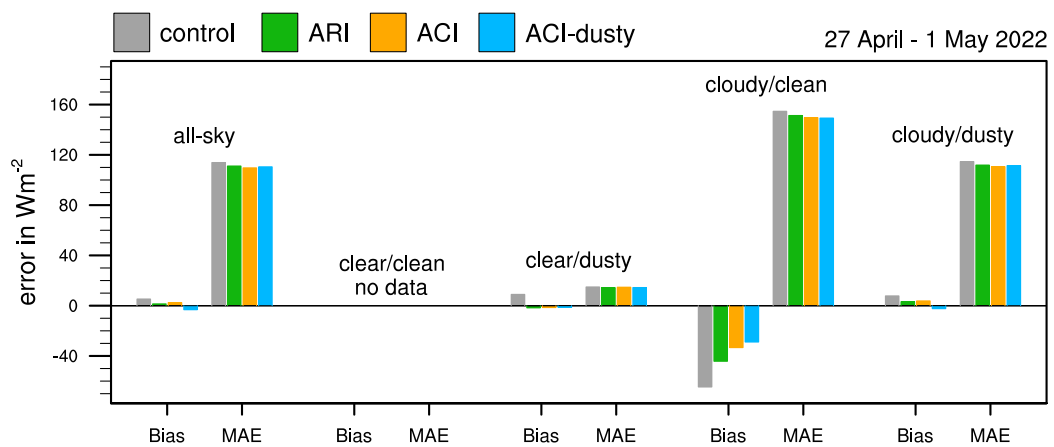
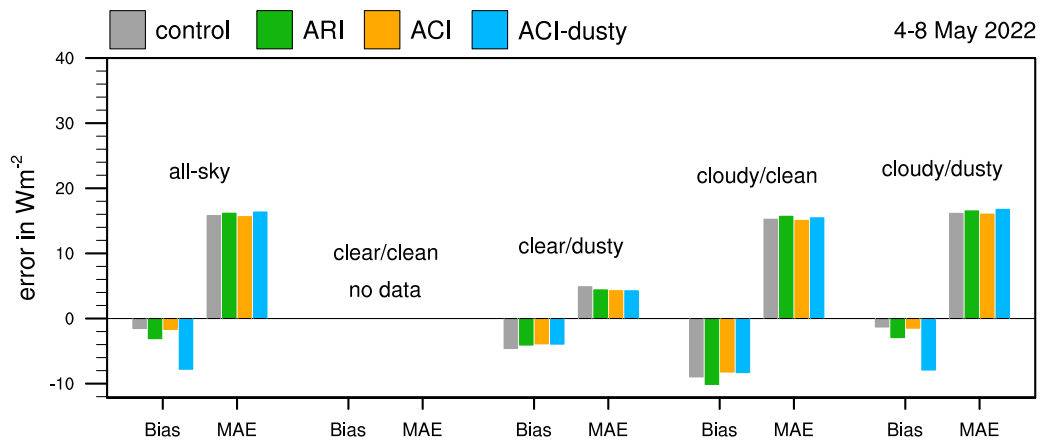
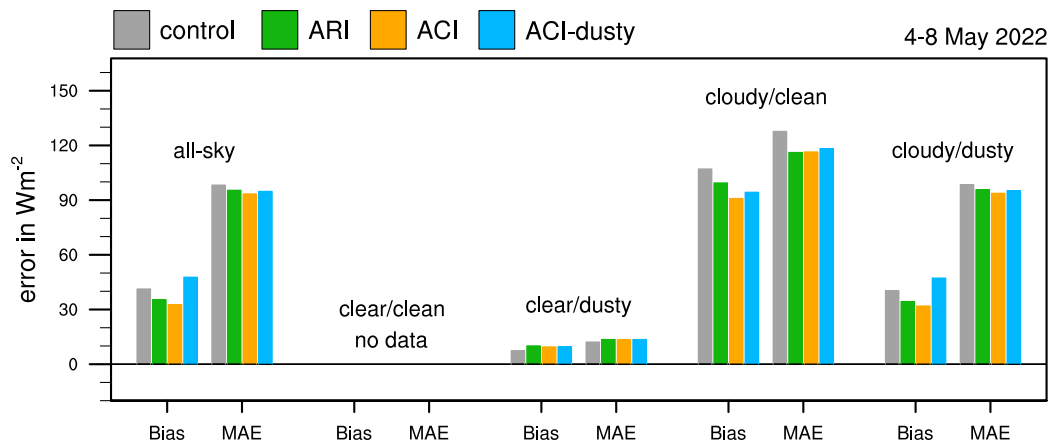


Figure S7. Bias and mean absolute error (MAE) of ICON-ART compared to CERES SSF level 2 radiative fluxes for 27 April to 1 May 2022. Shown are the outgoing longwave radiation at the top of atmosphere (TOA), the reflected shortwave at TOA and to solar irradiance at the surface (from top to bottom)

a) ICON-ART vs CERES outgoing longwave radiation at TOA



b) ICON-ART vs CERES reflected shortwave radiation at TOA



c) ICON-ART vs CERES downward shortwave radiation at the surface

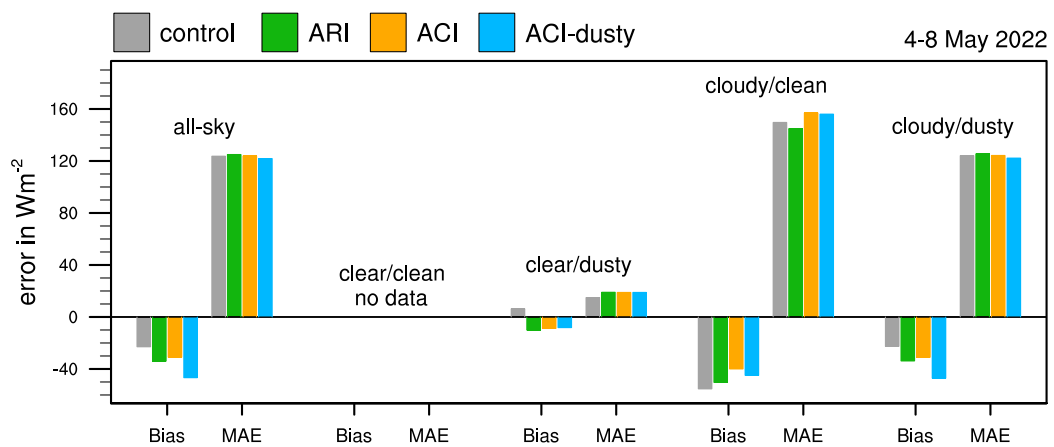
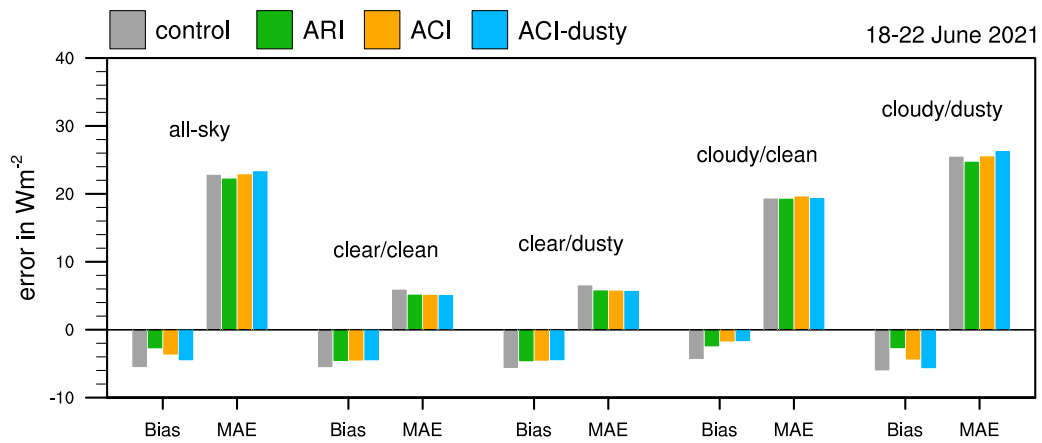
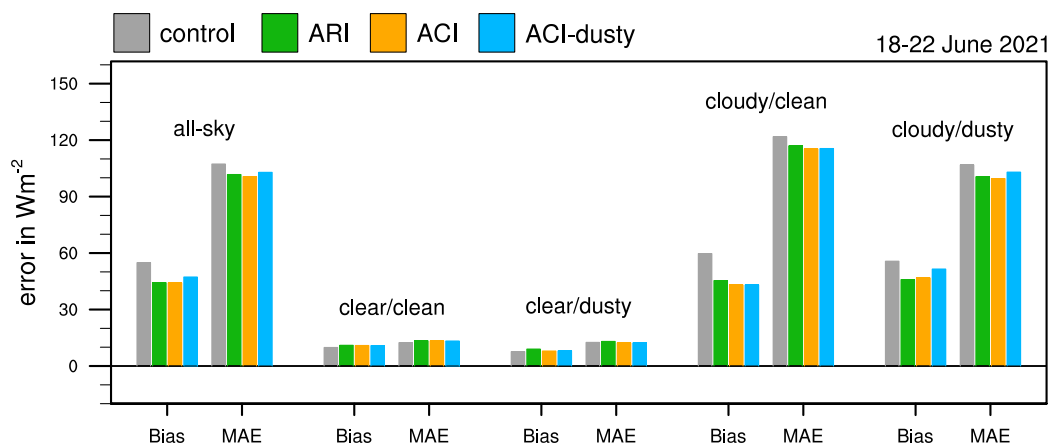


Figure S8. Bias and mean absolute error (MAE) of ICON-ART compared to CERES SSF level 2 radiative fluxes for 4-8 May 2022. Shown are the outgoing longwave radiation at the top of atmosphere (TOA), the reflected shortwave at TOA and to solar irradiance at the surface (from top to bottom)

a) ICON-ART vs CERES outgoing longwave radiation at TOA



b) ICON-ART vs CERES reflected shortwave radiation at TOA



c) ICON-ART vs CERES downward shortwave radiation at the surface

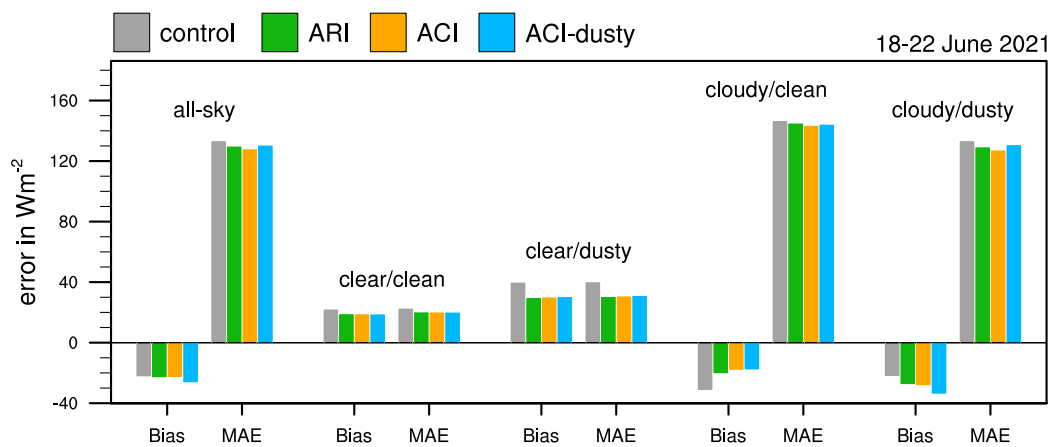
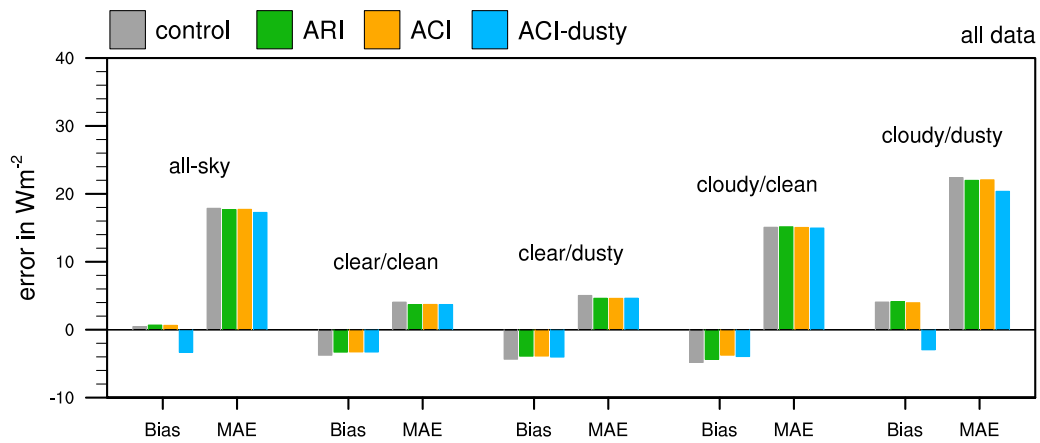
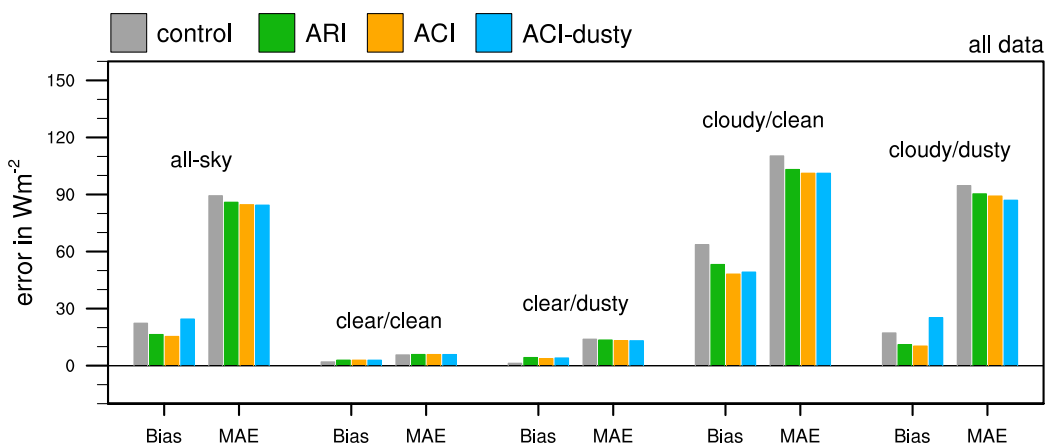


Figure S9. Bias and mean absolute error (MAE) of ICON-ART compared to CERES SSF level 2 radiative fluxes for 18-22 June 2021. Shown are the outgoing longwave radiation at the top of atmosphere (TOA), the reflected shortwave at TOA and to solar irradiance at the surface (from top to bottom)

a) ICON-ART vs CERES outgoing longwave radiation at TOA



b) ICON-ART vs CERES reflected shortwave radiation at TOA



c) ICON-ART vs CERES downward shortwave radiation at the surface

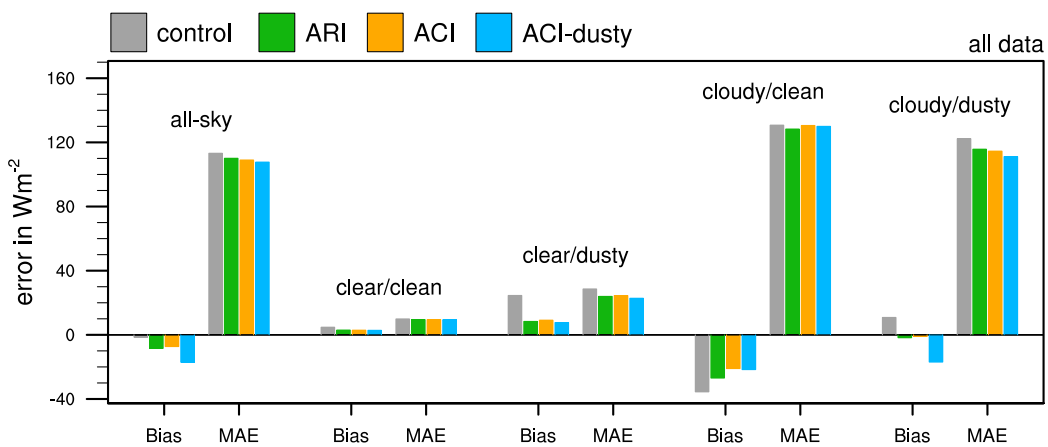


Figure S10. Bias and mean absolute error (MAE) of ICON-ART compared to CERES SSF level 2 radiative fluxes for all Saharan dust episodes. Shown are the outgoing longwave radiation at the top of atmosphere (TOA), the reflected shortwave at TOA and to solar irradiance at the surface (from top to bottom)

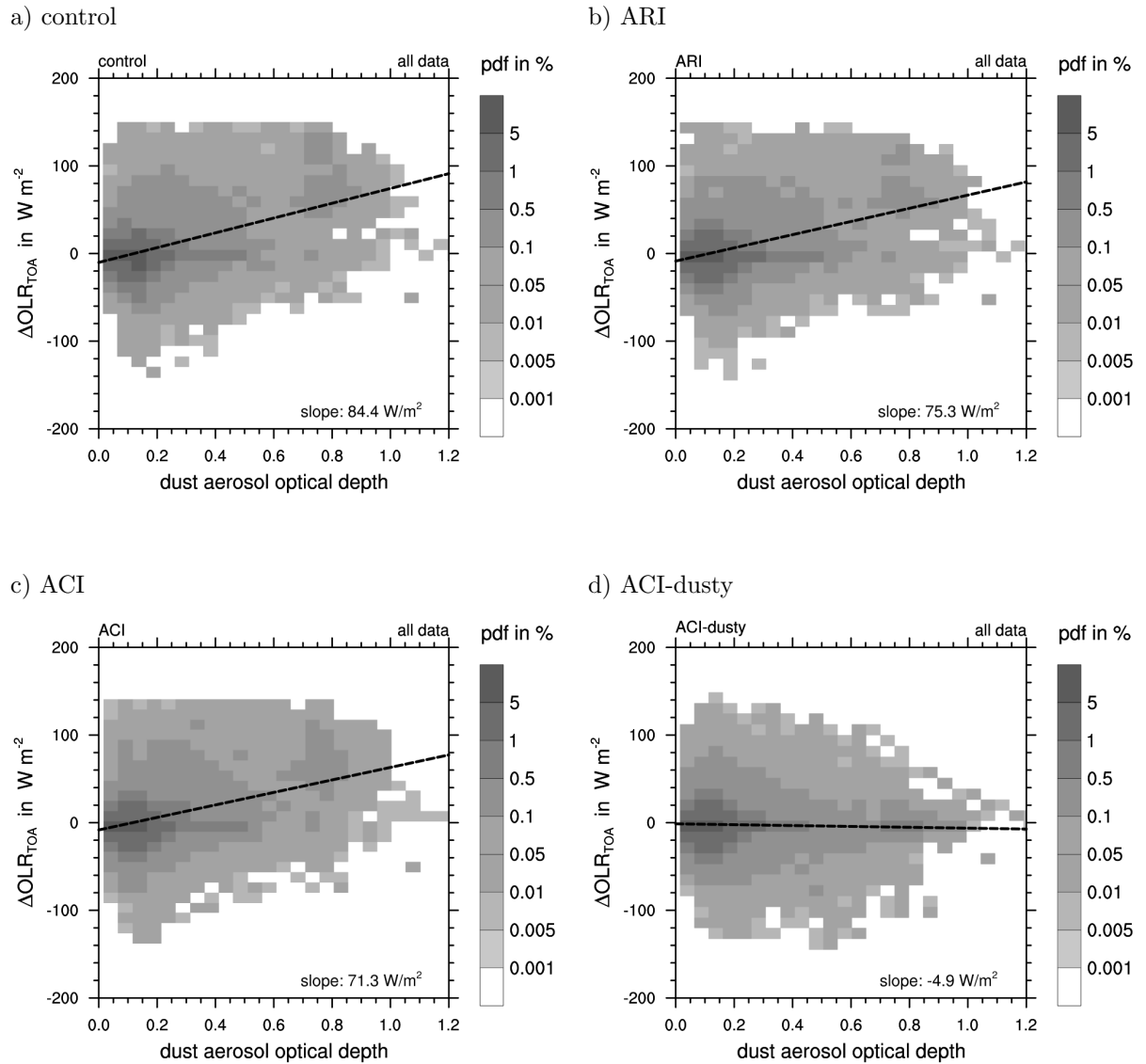


Figure S11. Joint histogram of errors in outgoing longwave radiation (OLR) as function of mineral dust AOD predicted by ICON-D2-ART for all six Saharan dust episodes. Errors are defined as (model-obs) for individual CERES footprints with a diameter of 25 km.

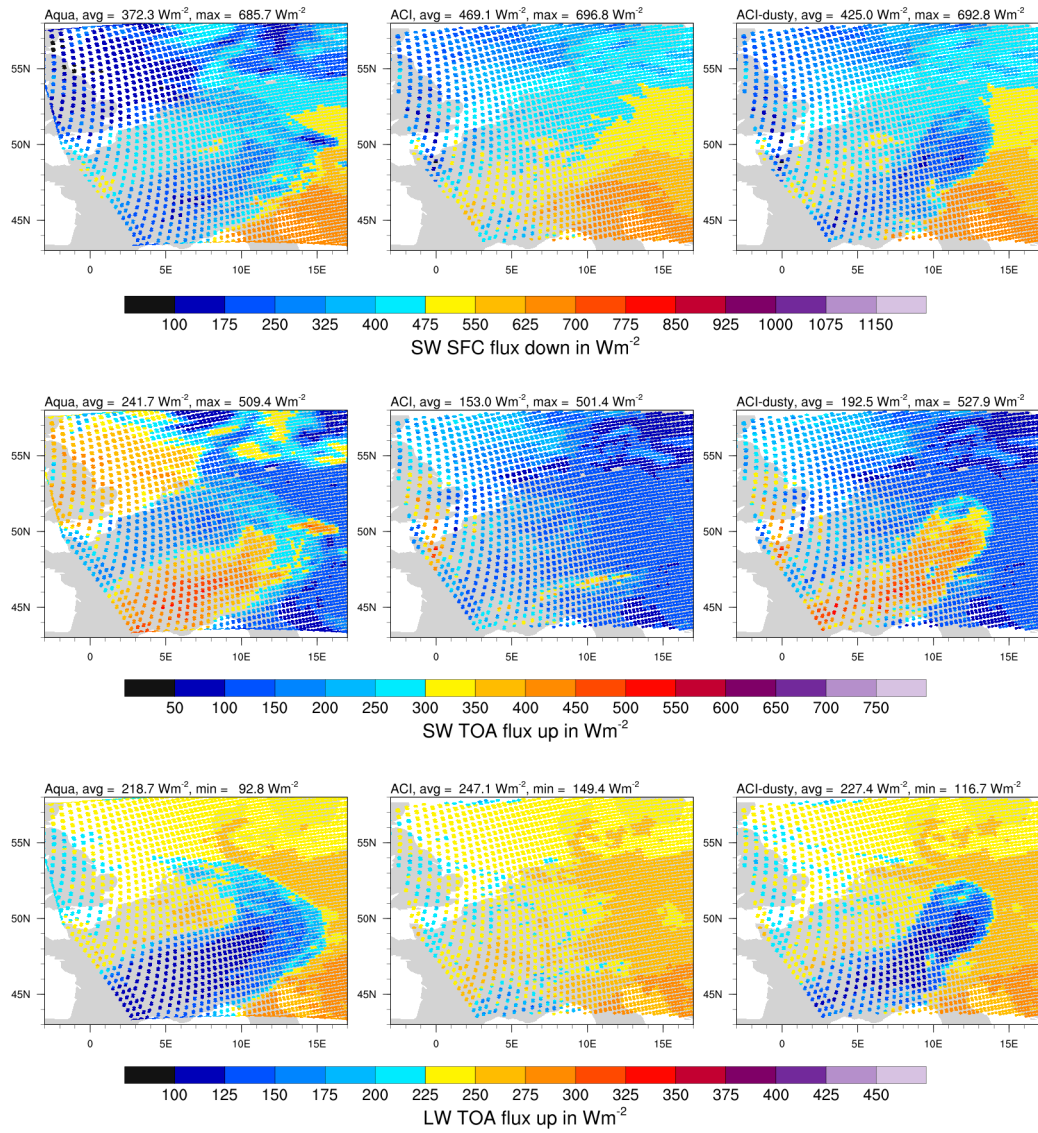


Figure S12. CERES SSF from Aqua vs ICON-D2-ART for 3 March 2021, 12:56 UTC.

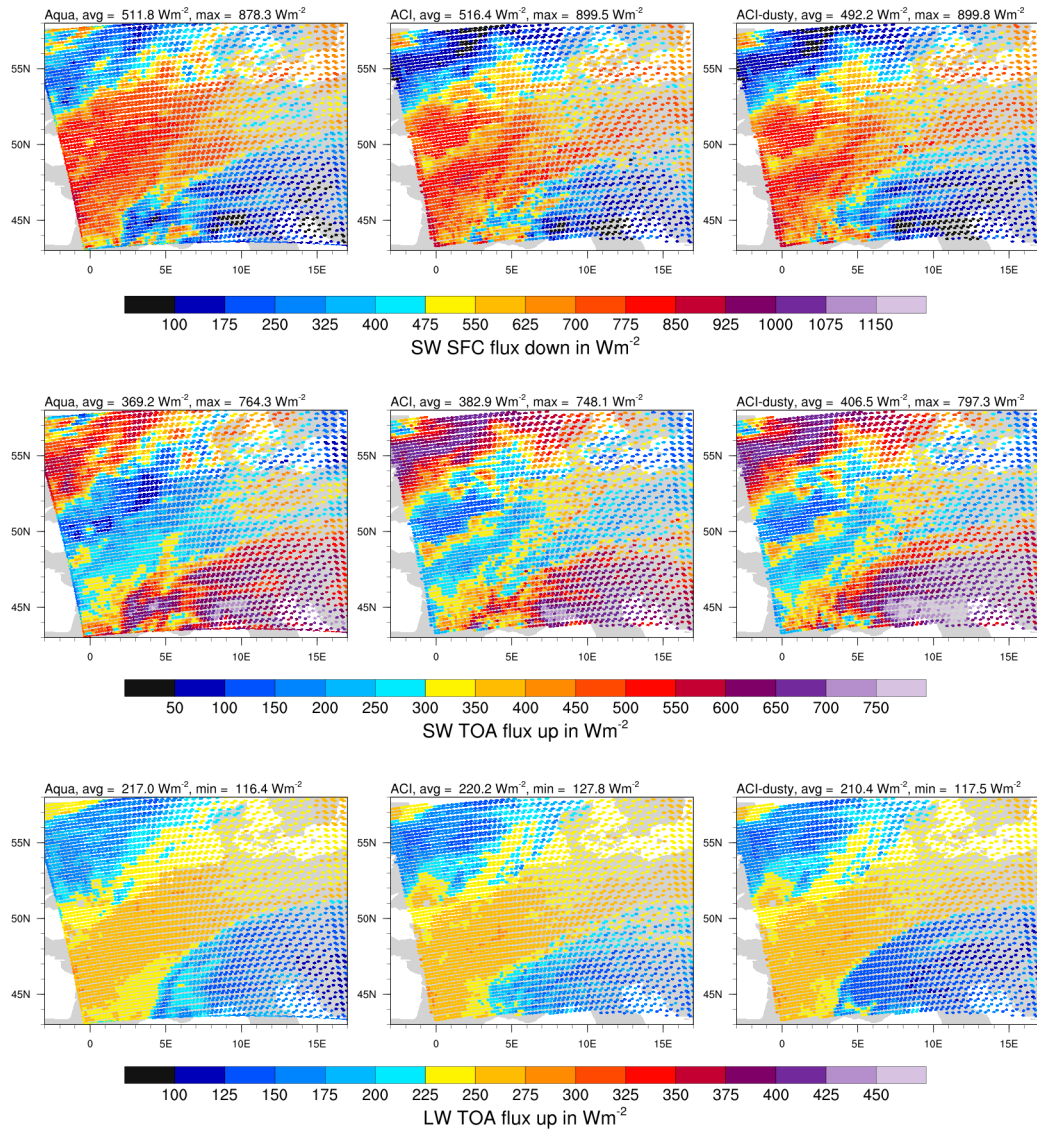


Figure S13. CERES SSF from Aqua vs ICON-D2-ART for 6 May 2022, 12:55 UTC.

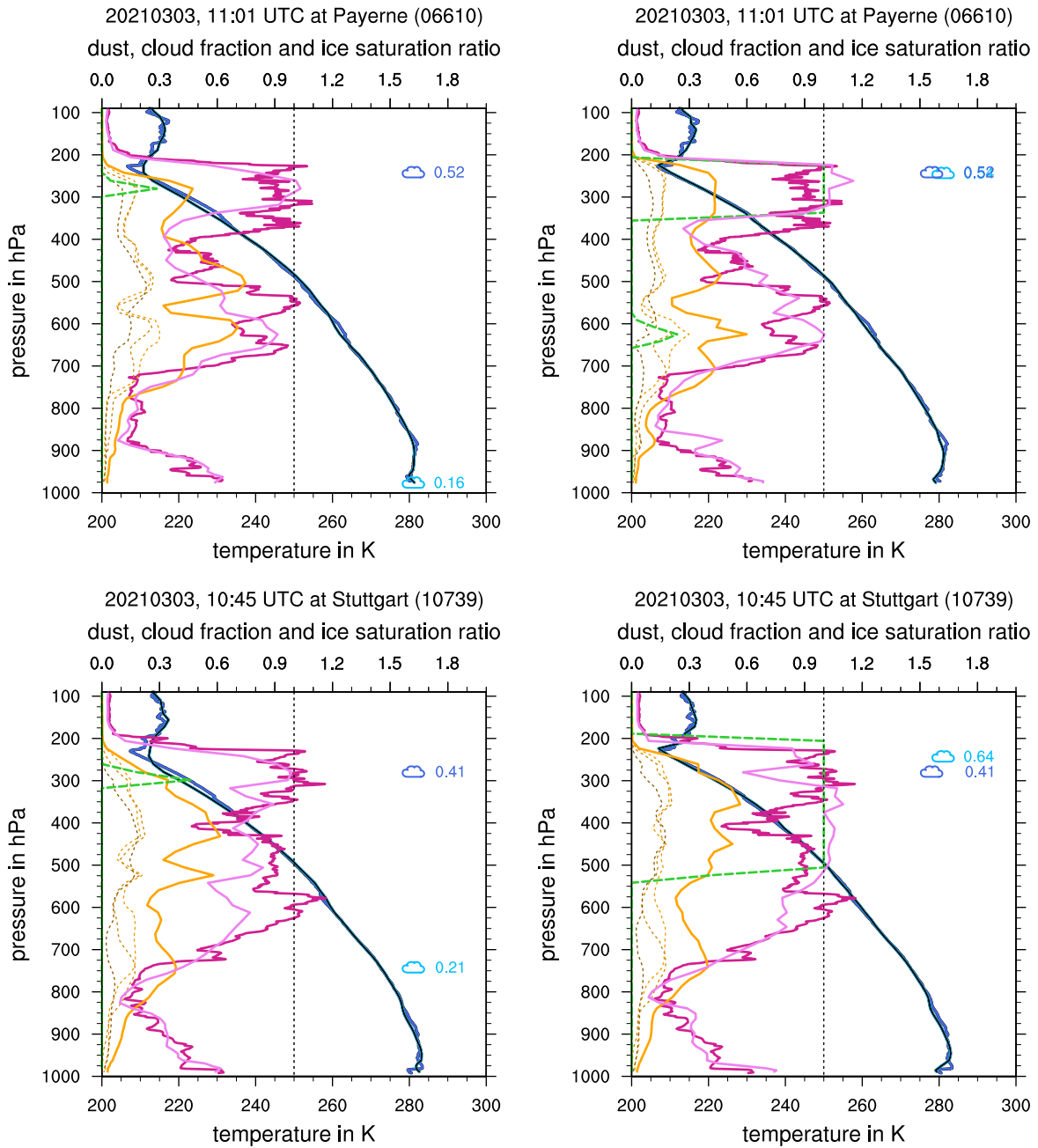


Figure S14. Vertical profiles from radiosonde measurements at Payerne, Switzerland (top) and Stuttgart, Germany (bottom) for 3 March 11 UTC and the corresponding ICON-ART profiles (top). Shown are ACI (left) and ACI-dusty (right). Observed temperature (black), ICON-ART temperature (blue), observed saturation ratio for ice (dark pink), ICON-ART saturation ratio (lighter pink), normalized total dust concentration of ICON-ART (thick orange), dust modes (other orange and browns), and ICON-ART cloud fraction (green). Cloud symbols indicate the SEVIRI BT (dark blue) and ICON-ART RTTOV BT (light blue) at 10.8 μm for this grid point. Numbers next to the cloud symbol give the visible reflectance.

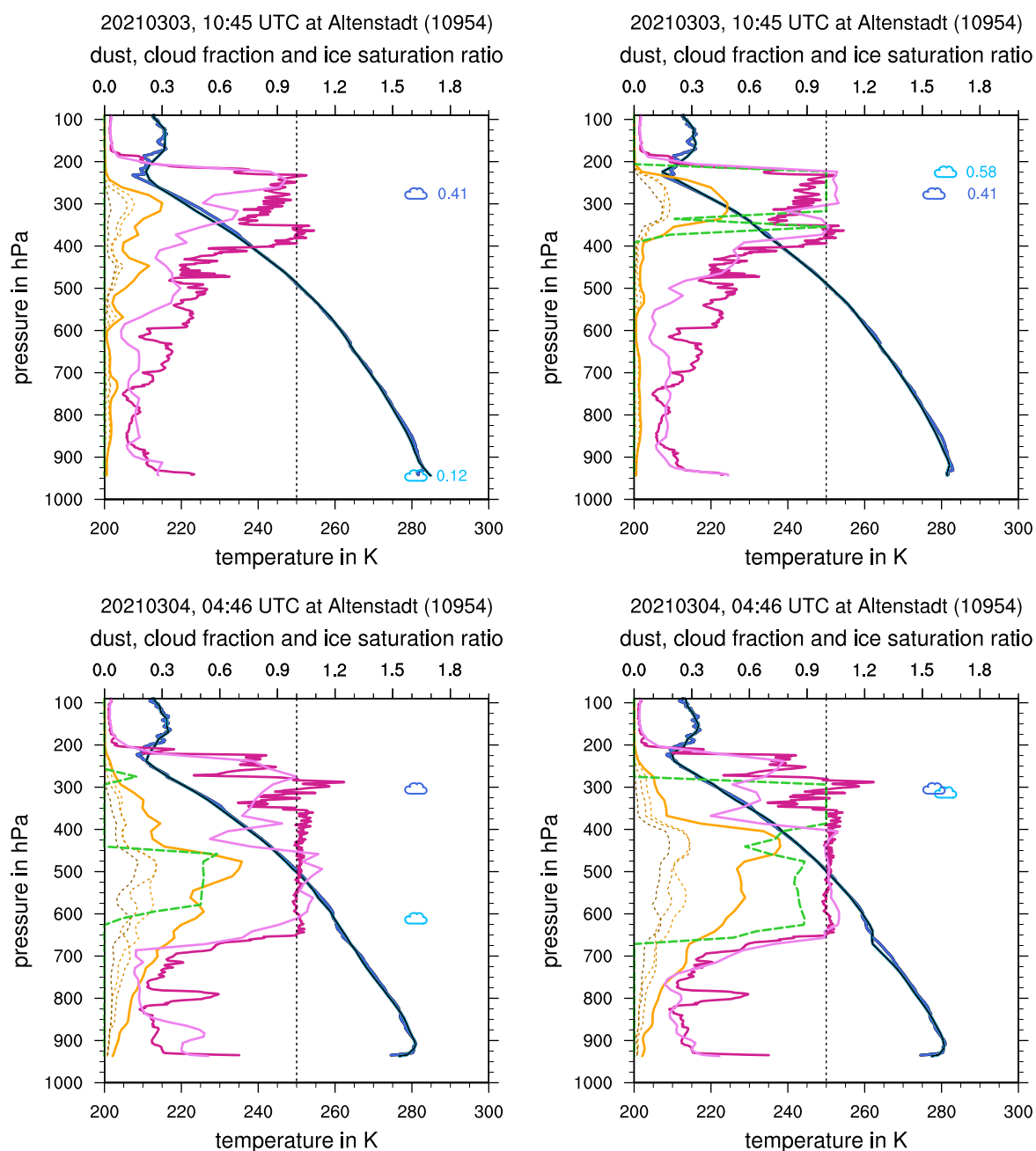


Figure S15. As previous figure, but for Altenstadt, Germany on 3 March 2021 11 UTC and 4 March 2021 5 UTC and the corresponding ICON-ART profiles. Shown are ACI (left) and ACI-dusty (right).

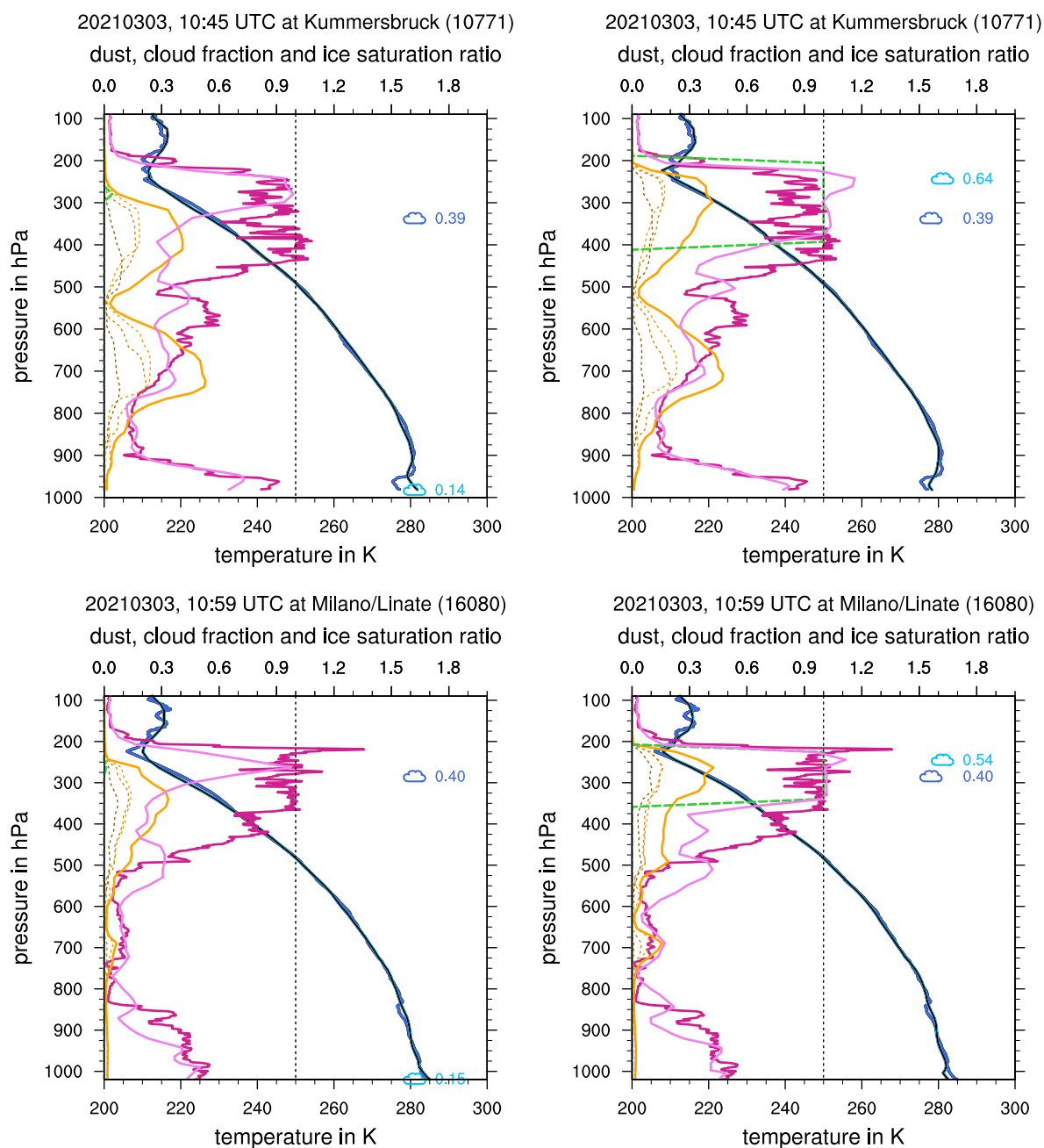


Figure S16. As previous figure, but for Kümmerbruck, Germany (top) and Milano, Italy (bottom) on 3 March 2021 11 UTC and the corresponding ICON-ART profiles. Shown are ACI (left) and ACI-dusty (right).